Neuron, Vol. 17, 1117–1131, December, 1996, Copyright ©1996 by Cell Press

PDGF Mediates a Neuron–Astrocyte Interaction in the Developing Retina

Marcus Fruttiger,* Andrew R. Calver,*
Winfried H. Krüger,† Hardeep S. Mudhar,*
David Michalovich,‡ Nobuyuki Takakura,§
Shin Ichi Nishikawa,§ and William D. Richardson*
*MRC Laboratory for Molecular Cell Biology
and Department of Biology
University College London
London WC1E 6BT
United Kingdom
†Department of Microbiology
and Program in Neurological Sciences
University of Connecticut Medical School
Farmington, Connecticut 06030-3205
‡Department of Experimental Pathology
United Medical and Dental Schools
Guy's Hospital Campus
London SE1 9RT
United Kingdom
§Department of Molecular Genetics
Faculty of Medicine
Kyoto University
Shogoin Kawaharacho 53
Sakyo-ku, Kyoto 606-01
Japan

Summary

Astrocytes invade the developing retina from the optic nerve head, over the axons of retinal ganglion cells (RGCs). RGCs express the platelet-derived growth factor A-chain (PDGF-A) and retinal astrocytes the PDGF alpha-receptor (PDGFRα), suggesting that PDGF mediates a paracrine interaction between these cells. To test this, we inhibited PDGF signaling in the eye with a neutralizing anti-PDGFRα antibody or a soluble extracellular fragment of PDGFRα. These treatments inhibited development of the astrocyte network. We also generated transgenic mice that overexpress PDGF-A in RGCs. This resulted in hyperproliferation of astrocytes, which in turn induced excessive vasculogenesis. Thus, PDGF appears to be a link in the chain of cell–cell interactions responsible for matching numbers of neurons, astrocytes, and blood vessels during retinal development.

Introduction

During development of the vertebrate eye, cells from several different sources come together in a coordinated fashion to form the final structure. The cells of the neural retina and pigmented epithelium are derived from the neural tube, whereas the eye lens is formed from the skin of the embryo as a result of inductive interactions between the skin epithelium and the underlying optic stalk. Other components of the eye, for example, the ciliary muscles and vascular system, are of mesenchymal or neural crest origin. For these diverse tissue elements to assemble correctly requires an intricate network of cell–cell communication. This is well illustrated by cell ablation experiments in transgenic mice. For example, if the cells of the eye lens are killed as they develop (by expressing a toxic gene product under the control of a lens-specific gene promoter), many other parts of the eye are secondarily affected and the whole eye is absent or much reduced in size (Kaur et al., 1989; Breitman et al., 1989; Landel et al., 1988). Likewise, ablating the pigmented epithelium has wide-ranging effects on development of the eye as a whole (Raymond and Jackson, 1995).

The retina itself is composed of cells with different developmental origins, whose numbers must presumably be matched to one another by cell–cell interactions. Most cells of the neural retina, such as photoreceptors, neurons, and Müller glia, are generated by multipotential neuroepithelial precursors that reside near the outer surface of the retina (Turner and Cepko, 1987; Wetts and Fraser, 1988; Holt et al., 1988; Turner et al., 1990). In contrast, retinal astrocytes originate from the optic stalk and migrate across the inner surface of the retina, starting from the optic nerve head around the day of birth (Stone and Dreher, 1987; Ling and Stone, 1988; Watanabe and Raff, 1988; Ling et al., 1989). The migrating astrocytes form a glial network that spreads radially in close association with the axons of retinal ganglion cells (RGCs). Patent blood vessels develop in the wake of the migrating astrocytes (Ling and Stone, 1988; Watanabe and Raff, 1988; Ling et al., 1989), presumably as a result of interactions between astrocytes and endothelial cells (Laterra et al., 1990; for a review, see Chang-Ling, 1994). Retinal astrocytes have been shown to make vascular endothelial cell growth factor (VEGF, also known as vascular permeability factor, VPF) (Alon et al., 1995), which is thought to be crucial for vascular development (Leung et al., 1989; Millauer et al., 1993; Peters et al., 1993; Stone et al., 1995; for a review, see Klagsbrun and Soker, 1993). However, the factors that control the astrocyte invasion of the retina and development of the astrocyte network are unknown.

We recently found that platelet-derived growth factor (PDGF) and its receptors are expressed in the developing rodent retina (Mudhar et al., 1993), suggesting that PDGF might be important in retinal development. PDGF is a covalent dimer of A- and B-chains (AA, BB, or AB) and exerts its biological effects through two closely related tyrosine kinase receptors (PDGFRα and PDGFRβ) (for review, see Heldin and Westermark, 1989). The two receptors have different ligand-binding specificities; PDGFRα binds all three dimeric isoforms of PDGF, while PDGFRβ binds PDGF-BB and, to a lesser extent, PDGF-AB, but not PDGF-AA. Cells in the walls of blood vessels in the retina (Mudhar et al., 1993) and elsewhere in the CNS (Smits et al., 1989; Koyama et al., 1994b) express PDGFRβ or PDGF-B (or both), suggesting that PDGF-BB might mediate local interactions among vascular cells. Furthermore, RGCs express PDGF-A and retinal astrocytes express PDGFRα, leading us to suggest that PDGF-AA might mediate a short-range paracrine interaction between RGCs and astrocytes during development (Mudhar et al., 1993).

To test this idea, we experimentally manipulated PDGF-A expression in the developing eye. We inhibited PDGF activity in vivo using a soluble extracellular fragment of PDGFRα that can neutralize the activity of all isoforms of PDGF and also with a neutralizing anti-PDGFRα monoclonal antibody. In both cases, development of the astrocyte network was retarded, strongly suggesting that PDGF mediates a developmental interaction between RGCs and astrocytes. In addition, we overexpressed PDGF-A in retinal neurons in transgenic mice. These transgenic animals displayed a striking hyperplasia of retinal astrocytes with their associated blood vessels, which, in older animals, bore a close resemblance to human proliferative retinopathy. These results emphasize the obligatory relationships among neurons, astrocytes, and vasculature in the retina, and suggest that PDGF is an important component of the signaling network that coordinates growth of these cells during development.

Results

Sequestering PDGF in the Developing Eye with the Extracellular Domain of PDGFRα Inhibits Formation of the Retinal Astrocyte Network

We wanted to test whether inhibiting PDGF signaling can inhibit normal development of the retinal astrocyte network. We therefore engineered a soluble extracellular fragment of PDGFRα as a neutralizing agent for all dimeric isoforms of PDGF (see Experimental Procedures) and inserted it into a replicating COS cell vector. A Myc epitope tag, recognized by monoclonal antibody 9E10 (Evan et al., 1985), was inserted in-frame with the truncated PDGFRα at its extreme carboxy terminus. The final construct was named pRα17, and the encoded polypeptide Rα17. The construct was electroporated into COS cells, which were fixed 72 hr later and labeled with monoclonal antibody 9E10. A proportion of the cells was labeled, giving intense intracellular labeling of the secretory apparatus (endoplasmic reticulum, Golgi apparatus, and cytoplasmic vesicles) (Pollock and Richardson, 1992; see Figure 2A). COS cells transfected with pRα17 were metabolically labeled with ^{35}S-amino acids and the cell lysate and supernatant were immunoprecipitated with monoclonal antibody 9E10, followed by polyacrylamide gel electrophoresis and autoradiography. The immunoprecipitates from both cell supernatant (Figure 1A, lane 1) and cell lysate (data not shown) contained high molecular weight polypeptides that were absent from control immunoprecipitations (lane 4). To test the PDGF-binding ability of the secreted Rα17 polypeptide, pRα17 and a similar plasmid encoding the short splice-variant of human PDGF-A (Pollock and Richardson, 1992) were electroporated separately into cultured COS cells, which were subsequently incubated with ^{35}S-amino acids. The cell culture media were collected and coincubated overnight at 4°C to allow PDGF-AA to bind to the truncated Rα17 receptor. The supernatants were then immunoprecipitated with an antiserum raised against pure human PDGF (R and D Systems). A large proportion of the PDGF-AA and the Rα17 truncated receptor coprecipitated in this experiment (Figure 1A, lane 2), demonstrating that the Rα17 polypeptide is capable of binding to PDGF-AA homodimers in solution, with an affinity high enough to withstand the physiological salt washes performed during the immunoprecipitation protocol.

To assess the ability of the Rα17 truncated receptor to inhibit the mitogenic effect of PDGF, NIH 3T3 cells were cultured in the presence of PDGF-AA, PDGF-BB, PDGF-AB, or basic fibroblast growth factor (bFGF) together with different concentrations of conditioned medium from COS cells expressing Rα17. DNA synthetic activity was measured by ^{3}H-thymidine incorporation. DNA synthesis induced by all three dimeric isoforms of PDGF was inhibited, in a dose-dependent manner, by COS cell medium containing Rα17 but not by control cell medium (Figure 1B). The mitogenic activity of bFGF was unaffected by Rα17. These results are consistent with the known ligand-binding properties of intact PDGFRα, which can bind and be activated by all three dimeric isoforms of PDGF (Heldin et al., 1988; Gronwald et al., 1988; Hart et al., 1988). The inhibitory effect of Rα17 on ^{3}H-thymidine incorporation could in turn be overcome by increasing the concentration of PDGF in the medium (data not shown), demonstrating that the PDGF-neutralizing effect of Rα17 is saturable. Under the conditions of our experiments, Rα17-conditioned medium neutralized between 1 and 3 ng/ml PDGF-AA. A similar truncated PDGFRα was previously shown to inhibit ligand-induced receptor phosphorylation (Yu et al., 1994).

COS cells, transfected with pRα17 and injected unilaterally into the eyes of newborn rats, persisted and continued to express the Myc-tagged Rα17 truncated receptor for several days in vivo (Figures 2B and 2C). Typically, they formed a compact bolus of cells that remained attached to the posterior surface of the lens. The size of the bolus indicated that the COS cells had continued to proliferate in the eye following injection. On postnatal day 5 (P5), injected and contralateral uninjected eyes were dissected and their retinae processed for whole-mount histochemistry with a monoclonal antibody against glial fibrillary acidic protein (GFAP, a specific marker for astrocytes). Eyes that showed signs of having been damaged by the injection procedure (e.g., blood in the vitreous) were rejected, as were eyes that did not appear to have a COS cell tumor and eyes in which the COS cells had invaded the retina (approximately half of the injected eyes were analyzed). There were no significant differences in the radii of retinae from eyes injected with mock-transfected COS cells versus uninjected eyes (data not shown), implying that the COS cells did not inhibit overall growth of the eye. In order to quantify the effect on astrocyte migration, the retinal whole-mounts were divided in six sectors and the distance of the most peripheral astrocyte to the optic nerve head was measured in each sector. The average of these six values was taken as a measure of the overall extent of the astrocyte network. For each experimental situation (pRα17-transfected COS cells, mock-transfected COS cells, contralateral eyes with no COS cell injections), nine

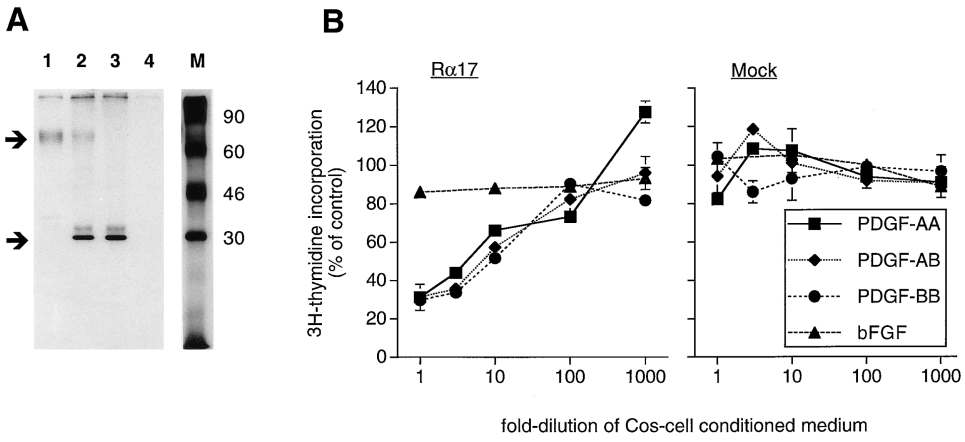

Figure 1. In Vitro Activity of Rα17 Truncated Receptor

(A) Immunoprecipitation of Rα17 truncated receptor bound to PDGF-AA. COS cells were electroporated with pRα17 or an analogous plasmid encoding PDGF-A and metabolically labeled with a ^{35}S-methionine/cysteine mixture. Cell culture supernatants were collected and immunoprecipitated, either with or without being previously coincubated overnight at 4°C with anti–PDGF-AA or 9E10 (anti-c-Myc) antibodies. Precipitates were run on a polyacrylamide gel and visualized by fluorography. Lane 1: Rα17-conditioned medium (CM) precipitated with anti-c-Myc. Lane 2: Rα17-CM, coincubated with PDGF-A-CM, precipitated with anti-PDGF-AA. Lane 3: Control (mock-transfected)-CM, coincubated with PDGF-A-CM, precipitated with anti-PDGF-AA. Lane 4: Rα17-CM precipitated with anti-PDGF-AA. Lane M: molecular weight markers. Upper arrow: position of Rα17 polypeptide. Lower arrow: position of plasmid-encoded PDGF-AA. A proportion of Rα17 and PDGF-AA coprecipitate with anti-PDGF-AA (lane 2).

(B) Neutralization of PDGF isoforms with Rα17 truncated receptor. Subconfluent cultures of NIH 3T3 cells were growth-arrested by serum deprivation. Purified growth factors were added to a fixed concentration, sufficient to stimulate half-maximal mitogenic response, together with different dilutions of conditioned medium from COS cells that had been transfected with plasmid pRα17 (left panel, "Rα17") or with the vector backbone alone (right panel, "mock"). After overnight incubation at 37°C, ^{3}H-thymidine was added to the cultures for 4 hr before solubilizing the cells and determining the amount of TCA-precipitable radioactivity by scintillation counting. Assays were performed in triplicate. The results are expressed as a percentage of the incorporation obtained in response to growth factor alone. Conditioned medium containing Rα17 truncated receptor was able to neutralize all three dimeric isoforms of PDGF, but not bFGF, in a dose-dependent fashion. For further details, see Experimental Procedures.

retinae were examined. Careful observation revealed a slight rotational asymmetry in the normal distribution of astrocytes in uninjected eyes at P5. In retinae from eyes that had been injected with mock-transfected COS cells, the GFAP immunoreactivity reflected the normal distribution of astrocytes (Figure 2D). The radius of the astrocyte network (estimated as described above) was only slightly reduced, by 5% ± 3.9% (mean ± SD, n = 9), in mock-transfected COS cell–injected eyes when compared with contralateral uninjected eyes.

In retinae from eyes that had received COS cells expressing Rα17, development of the astrocyte network was clearly perturbed (Figure 2E). The effect was not uniform across the retina, being greater in one half of the retina than the other. In those retinal sectors that were most affected, the morphology of the network was altered (compare Figures 2D and 2E), having a less intricate branching pattern compared with control retinae. In addition, the extent of the retinal astrocyte network was dramatically reduced in the more affected half of the retina. To quantify this effect, we compared the radial distances covered by astrocytes in the two most affected sectors of each retina that was exposed to pRα17-transfected COS cells with the two shortest distances measured in each retina that was exposed to mock-transfected COS cells; we found a reduction in the Rα17-treated retinae of 31% ± 9.6% (n = 9, $p < 0.01$ Student's t-test). However, part of these measured distances had already been traveled by the astrocytes before birth, prior to the COS cell injections. When the extent of the astrocyte network in normal newborn rats was subtracted, we found that the distance migrated by astrocytes *during the course of the experiment* was reduced by 51% ± 18.3% (n = 9) as a result of exposure to Rα17.

Systemically Delivered Anti-PDGFRα Immunoglobulin Perturbs Development of the Retinal Astrocyte Network

As another means of inhibiting PDGF signaling, we used a rat monoclonal anti-mouse PDGFRα (antibody APA5) that competes with PDGF-AA and PDGF-BB for binding to PDGFRα on Balb/c-3T3 cells (Takakura et al., 1996) and inhibits PDGF-AA-induced responses in Balb/c-3T3 cells and cultured fetal liver cells (N. T., unpublished data). Newborn mice were injected subcutaneously with 50 μg of column-purified APA5 Ig once each day for 3 days, then they were processed for whole-mount immunohistochemistry with anti-GFAP and anti-collagen IV. Littermates that had been injected with 50 μg of monoclonal rat anti-mouse c-Kit Ig (antibody ACK2) or with vehicle alone served as controls. To test whether the subcutaneously injected antibodies reached the eye and bound to retinal astrocytes, we performed whole-mount immunohistochemistry with FITC-conjugated goat-anti-rat IgG (Figures 3A–3C). In mice injected with APA5, the

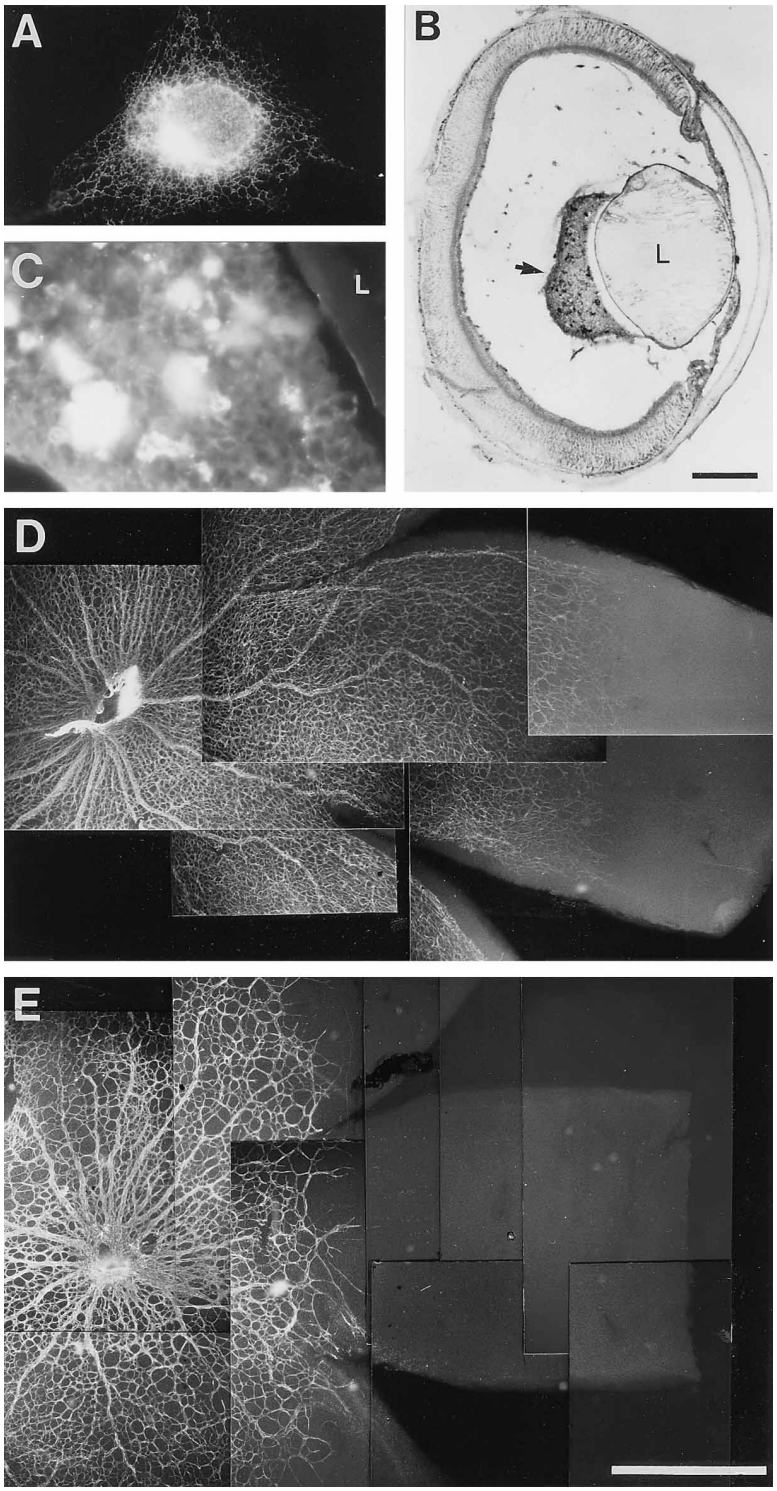

Figure 2. Neutralizing PDGF with an Extracellular Fragment of the PDGFRα Inhibits Formation of the Retinal Astrocyte Network during Normal Development

(A) Immunofluorescence micrograph of a COS cell transfected with pRα17 (see Experimental Procedures) and labeled in vitro with monoclonal 9E10 and fluorescent secondary antibodies.

(B) Micrograph of a cryosection through an eye containing an implant of COS cells that were transfected with pRα17. The cells were injected at P0 and the eye processed for micrography on P5. The arrow points to the bolus of COS cells adhering to the back of the lens (L). The dark granules within the COS cell mass are Rα17-expressing cells visualized by 9E10 immunolabeling followed by an immunoperoxidase detection system.

(C) High magnification micrograph of a COS cell mass like that in (B), labeled with antibody 9E10 followed by fluorescent secondary antibodies. Isolated cells or clusters of cells within the cell mass label strongly for Rα17 truncated receptor.

(D) and (E) Composite immunofluorescence micrographs of whole-mount retinae, labeled with anti-GFAP to visualize the retinal astrocyte network.

(D) Part of a normal P5 retina.

(E) Part of a retina from an eye injected at P0 with COS cells expressing Rα17 and processed for micrography at P5. The extent of the astrocyte network is much reduced and the fine structure of the network is coarser. Scale bars, 500 μm.

anti-rat IgG-FITC conjugate clearly outlined the astrocyte network (Figure 3A), whereas in mice treated with ACK2 or PBS, no staining above background was observed (Figures 3B and 3C). Mice treated with ACK2 showed reduced skin pigmentation as described previously (Nishikawa et al., 1991), indicating that the control antibody was active. We were able to localize rat IgG immunoreactivity in ACK2-injected mice on an unidentified subset of retinal cells located near the optic nerve head at P5 (data not shown), demonstrating that ACK2 had reached the retina.

The retinal astrocyte network (revealed by GFAP immunolabeling) in P3 mice injected with APA5 was strikingly perturbed in morphology and reduced in radial

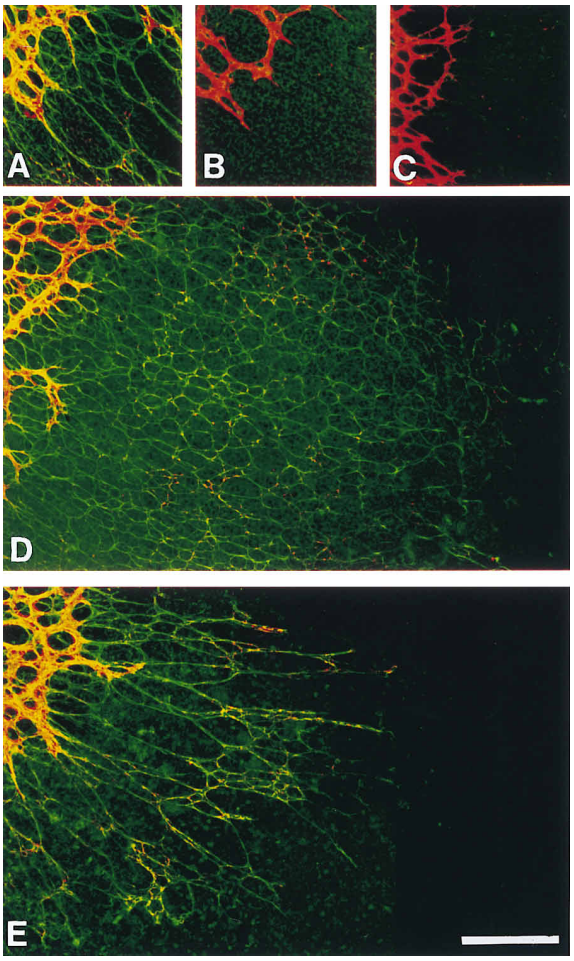

Figure 3. Anti-PDGFRα Neutralizing Antibodies Inhibit Normal Development of the Retinal Astrocyte Network

(A)–(C) Retinae of mice that were injected subcutaneously in the neck each day from birth to P3 with rat-anti-mouse PDGFRα Ig (A), rat-anti-mouse c-Kit Ig (B), or vehicle alone (C), then fixed and labeled with fluorescein-conjugated goat-ant-rat Ig (green). The sections were also labeled with anti-collagen IV and rhodamine-conjugated second antibodies (red). Small sections of the retinae at the leading edge of the developing vascular net are shown. In each case, the optic nerve head is outside the field of view to the left. The anti-PDGFRα Ig clearly entered the living retina and bound to the surfaces of astrocyte processes (A). No anti-rat IgG staining can be detected in mice injected with anti-c-Kit antibody (B) or vehicle alone (C).

(D) and (E) Mouse retinae injected with anti-c-Kit Ig (D) or anti-PDGFRα Ig (E) as above, fixed and double-labeled for GFAP (green), and collagen IV (red). Note the reduced and distorted astrocyte network in anti-PDGFRα-injected mice (E) compared with the normal appearance of the astrocyte network in anti-c-Kit-injected mice (D). Scale bar, 200 μm.

spread when compared with control retinae from ACK2-injected mice (Figures 3D and 3E). The ACK2 injections had no effect on the retinal astrocyte network when compared with retinae from mice injected with vehicle alone. In APA5-injected mice, the astrocytes seemed to be more fasciculated and possibly reduced in numbers, because the astrocyte network had a more open mesh than normal (Figure 3). As in the Rα17 experiment described above, the effect was more pronounced in one half of the retina than in the other. It is likely that inherent asymmetrical properties of the developing retina are the root cause of the uneven effect of systemic APA5 injection (and, by extrapolation, Rα17 treatment too). In addition to the disturbed morphology of the astrocyte network found in APA5-injected mice, there was also a reduction in the extent of astrocyte migration. Combining data from three independent experiments, the average radial distance migrated over all six sectors of the APA5-treated retinae ($n = 13$) was reduced by 20% $\pm$ 1.2% compared with ACK2-treated retinae ($n = 10$).

There is believed to be a close link between the development of retinal astrocytes and blood vessels (see below), so we also examined the retinal vasculature in APA5-injected eyes. There was possibly a small inhibitory effect on the vasculature, but this was much less pronounced than the effect on astrocytes and we did not attempt quantitation. Vascular cells do not express PDGFRα so a direct effect of the antibody on these cells is not expected.

Transgenic Mice That Overexpress PDGF-A in Neurons

We generated transgenic mice that express PDGF-A in subsets of central and peripheral neurons under transcriptional control of the rat neuron-specific enolase (NSE) gene promoter (Forss-Petter et al., 1990). The transgene contained a human PDGF-A cDNA engineered to encode the "short" alternative-splice isoform of PDGF-A with a Myc epitope tag appended to the carboxy terminus (hPDGF-A; Figure 4A) (Pollock and Richardson, 1992). The "short" PDGF-A isoform is freely diffusible in the extracellular fluid, since it lacks the extracellular matrix-binding motif present at the carboxy terminus of the "long" PDGF-A isoform (LaRochelle et al., 1991; Östman et al., 1991; Khachigian et al., 1992; Pollock and Richardson, 1992; Raines and Ross, 1992). In addition to the NSE-PDGF-A mice, we also generated transgenic mice expressing a closely related transgene encoding an endoplasmic reticulum (ER)-retained form of hPDGF-A (PDGF-A_{KDEL}; Figure 4A). Seven NSE-PDGF-A founders and four NSE-PDGF-A_{KDEL} founders were obtained. Four of the NSE-PDGF-A founders (A5-64, -72, -75, -82) and all of the NSE-PDGF-A_{KDEL} founders (A10-3, -21, -23, -26) transmitted the transgene to their first offspring and transgenic lines were established. The transgene copy numbers of the lines were all in the range 1–10; the line used for all the experiments described in this paper (A5-75) had about five transgene copies per genome. We used a reverse transcriptase (RT)–PCR approach to examine expression of transgene-derived hPDGF-A mRNA in the retinae of each line (e.g., Figure 4B). The PCR primers were chosen to amplify PDGF-A transcripts across the Myc epitope sequences near the 3′ end of the transgene. Thus, transgene-derived human PDGF-A transcripts could be distinguished unambiguously from endogenous mouse transcripts by the size of the PCR product after Southern blotting and probing with a PDGF-A-specific oligonucleotide. Reprobing the Southern blot with

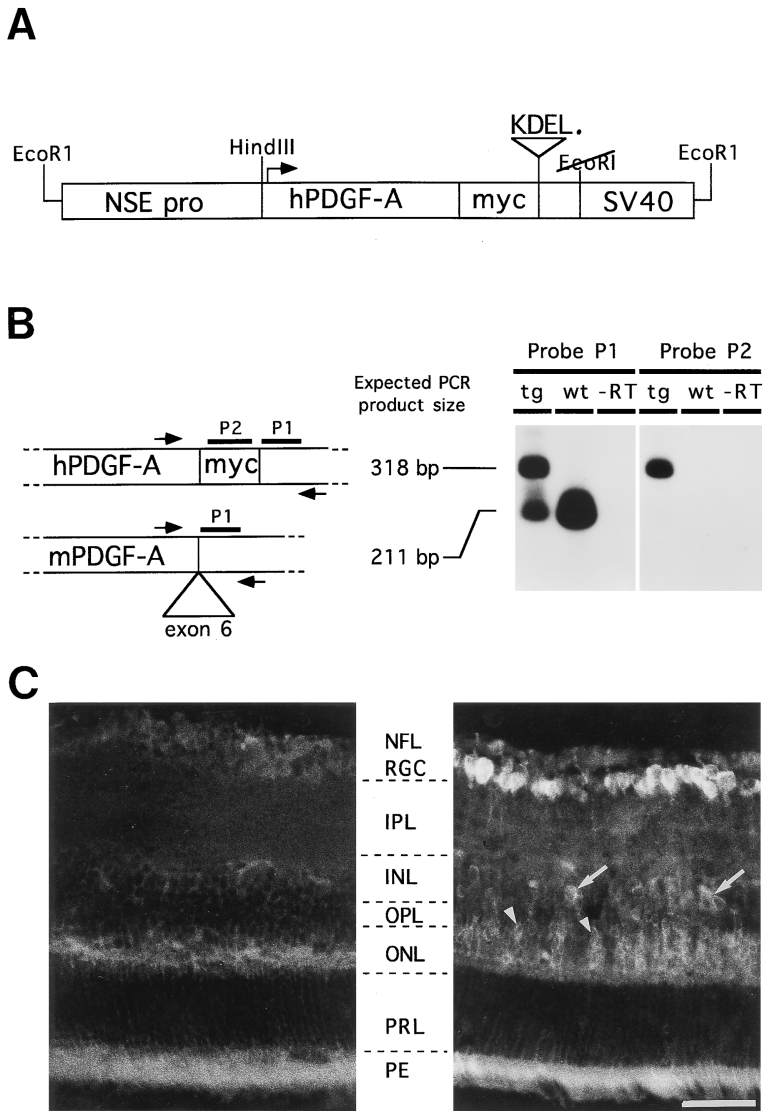

Figure 4. Structure and Expression of the Human PDGF-A Transgene

(A) The transgene consists of human PDGF-A coding sequences (1.0 kb) with a Myc epitope tag (44 bp) at its carboxy terminus, under the control of the rat NSE gene promoter (1.8 kb) and SV40 polyadenylation site. A second closely related transgene also had an oligonucleotide encoding an endoplasmic reticulum (ER) retention signal followed by a stop codon (KDEL.) inserted immediately downstream of the Myc tag. See Experimental Procedures for construction details.

(B) Expression of transgene-derived mRNA was detected by RT–PCR. Left, diagram showing the predicted structures of the transgenic (hPDGF-A) and endogenous (mPDGF-A) mRNAs, and the relative positions of oligonucleotide PCR primers (arrows) and hybridization probes (P1, P2) used for detection. The position of exon 6 (69 bp), which encodes an extracellular matrix binding motif that can be inserted by alternative splicing, is indicated. Right, agarose gel electrophoresis of RT–PCR products generated from line A5-75 transgenic (tg) or wild-type (wt) P3 retinae and a control reaction (−RT) in which reverse transcriptase was omitted from the PCR reaction, Southern blotted, and probed with ^{32}P-labeled probes P1 (detects all PDGF-A mRNA species) or P2 (detects only transgene-derived mRNA). The predicted sizes of the PCR products are 211 bp ("short" mPDGF-A mRNA lacking exon 6), 280 bp ("long" mPDGF-A mRNA including exon 6), or 318 bp (transgenic hPDGF-A mRNA). A series of control experiments established that our RT–PCR reaction conditions were such that the band intensities after blotting were proportional to the amount of mRNA added; band intensities could therefore be compared on a semiquantitative basis. Densitometry of gel lanes indicated that there were about five times as many transgene-derived PDGF-A transcripts as endogenous transcripts in the neural retina of line A5-75, and also that no "long" form mPDGF-A mRNA can be detected in wild-type or transgenic retinae.

(C) Immunofluorescence localization of transgene-derived hPDGF-A in the retina of a P14 transgenic mouse expressing the ER-retained form of hPDGF-A (see [A]). Monoclonal 9E10 (anti-c-Myc) was the primary antibody; FITC-conjugated rabbit-anti-mouse IgG was the secondary antibody. The transgenic retina is on the right, a wild-type littermate on the left. The strongest signal is detected in the cell bodies of retinal ganglion cells (RGC); a weaker signal is detected in the cell bodies of photoreceptor cells in the outer nuclear layer (ONL, arrowheads), and in the inner nuclear layer (INL, arrows). The strong signal in the pigment epithelium (PE) is background autofluorescence. Retinal astrocytes migrate into the retina along the plane of the nerve fibre layer (NFL), which contains the projection axons of RGCs. IPL, inner plexiform layer; OPL, outer plexiform layer; IS, OS inner and outer segments of the photoreceptor cells. Scale bar, 50 μm.

a specific *c-myc* oligonucleotide provided further proof of the transgenic derivation of the transcripts (Figure 4B). Three of the four NSE-PDGF-A transgenic mouse lines and two of the four NSE-PDGF-A_{KDEL} lines expressed transgene-derived mRNA (data not shown). We quantified the mRNA expression level in hemizygous mice of line A5-75 by densitometry of Southern blots in a BioRad Molecular Imager (see Experimental Procedures). At birth, P3, and P14, there were between five and seven times more transgene-derived hPDGF-A transcripts than endogenous transcripts in the neural retinae of these mice. Expression of both transgenic and endogeneous PDGF-A declined somewhat in the adult, although transgenic PDGF-A was still more abundant.

We were unable to detect any immunoreactivity over background in retinae from any of the NSE-PDGF-A mice using antibody 9E10, which recognizes the Myc epitope present in the transgene-encoded hPDGF-A. However, in both of the NSE-PDGF-A_{KDEL} lines, we could easily visualize the encoded polypeptide in the cell bodies of RGCs and, at a lower level, in neurons in the inner and outer nuclear layers (Figure 4C). The protein was abundant in all RGCs from before the day of birth (data not shown) to at least the end of the second postnatal week (Figure 4C) and was still expressed, at a lower level, in the adult (data not shown). The spatial expression pattern, in particular expression in RGCs, was similar to that previously described for an NSE-*lacZ* transgene

(Forss-Petter et al., 1990; Seiler and Aramant, 1995) and an NSE-BCL2 transgene (Martinou et al., 1994), demonstrating that the activity of the NSE promoter cassette is not markedly affected in *cis* by flanking chromosomal sequences at the site of integration. Thus, it seems very likely that the expression pattern of the PDGF-A_{KDEL} transgene is a faithful representation of the expression pattern of the secreted PDGF-A transgene. We conclude, therefore, that our NSE-PDGF-A transgenic mice synthesize the encoded PDGF polypeptide in RGCs and other retinal neurons but that this does not accumulate to a detectable degree either inside cells or in the extracellular space following secretion. This conclusion is strongly supported by phenotypic analysis of the NSE-PDGF-A mice (see below). Note that the expression pattern of transgene-derived PDGF-A is not dissimilar to the endogenous pattern of PDGF-A expression (Mudhar et al., 1993). Both are expressed in the great majority of RGCs, with no noticeable gradient of expression from central-to-peripheral at postnatal ages. Endogenous PDGF-A is also expressed in a subset of amacrine neurons in the inner nuclear layer, whereas transgenic PDGF-A is expressed in neurons in both the inner and outer nuclear layers.

The RT–PCR assay was also able to distinguish between endogenous mouse mRNAs that encoded the "short" and "long" alternative splice isoforms of PDGF-A. Only the "short" isoform was detected in wild-type or transgenic mice, demonstrating that only this isoform is normally produced in the P3 mouse retina.

Hyperplasia of the Retinal Astrocyte Network in NSE-PDGF-A Mice

During normal development, retinal astrocytes migrate radially across the inner surface (i.e., the nerve fiber layer) of the retina from the optic nerve head, starting around the day of birth and reaching the periphery of the retina around postnatal day 5 (P5) in the rat and the mouse (Watanabe and Raff, 1988; Mudhar et al., 1993; M. F., unpublished data). Since retinal astrocytes express PDGFRα (Mudhar et al., 1993), which can be activated by all three dimeric isoforms of PDGF (AA, AB, BB), we expected that development of retinal astrocytes might be perturbed in the NSE-PDGF-A mice. Immunohistochemistry with antibodies against GFAP revealed that all three transgenic lines that expressed transgene-derived mRNA displayed hyperplasia of the retinal astrocyte network (Figure 5). The fourth NSE-PDGF-A line (A5-72) that did not express the transgene had no phenotype (data not shown), demonstrating a correlation between transgene expression (at the mRNA level) and phenotype. It is noteworthy that neither of the two NSE-PDGF-A_{KDEL} transgenic lines had any retinal phenotype, despite the fact that the ER-retained PDGF-A accumulated to a high level in RGCs of these mice (Figure 4C). This provides strong genetic evidence that the phenotype of the NSE-PDGF-A mice depends on the ability of the transgene-derived PDGF protein to be secreted from the cells that synthesize it.

We investigated the transgene dose dependence of the retinal astrocyte phenotype of NSE-PDGF-A mice by comparing hemizygous and homozygous transgenic littermates of one of the lines, called A5-75. At P4, the homozygous animals displayed a retinal astrocyte phenotype that was clearly more severe than that of the hemizygotes (Figures 5B and 5C). The homozygotes (which have a double complement of transgenes and, presumably, correspondingly higher PDGF-A expression) had a much denser mat of $GFAP^+$ astrocyte processes than either the hemizygotes or wild-types (Figures 5A–5C). The radial spread of astrocytes from the optic nerve head was less in the homozygotes than in the hemizygotes at P4, and less in the hemizygotes than in wild-type mice (Figures 5A–5C). At P4, for example, the average radius of the astrocyte net was reduced by 41% $\pm$ 10.6% (n = 10) in heterozygotes and by 59% $\pm$ 1.3% (n = 5) in homozygotes compared with wild type. Possible reasons for this effect are discussed later. However, despite the fact that astrocyte migration was retarded in A5-75 mice during early postnatal development, the astrocytes did eventually reach all the way to the periphery of the transgenic retinae.

Hypervascularization of the Retina in NSE-PDGF-A Transgenic Mice

It is known that astrocytes influence retinal vasculogenesis during normal development (see Discussion), so we predicted that the increased number of astrocytes in NSE-PDGF-A transgenic retinae might in turn induce overproduction of blood vessels. We used antibodies against GFAP and collagen IV to specifically label astrocytes and blood vessels (Herken et al., 1990; Connolly, 1991), respectively. We compared the gliovascular nets in retinae of P4 wild-type, hemizygous, and homozygous transgenic (A5-75) animals (Figures 5D–5F). There was a striking correspondence between the astrocyte and vascular nets in all three genotypes; not only was there transgene dose-dependent overproduction of blood vessels in the transgenic retinae, but the distribution of vessels closely matched the distribution of astrocyte processes; that is, the vessels did not spread further than the astrocytes. The correspondence between astrocytes and blood vessels is particularly obvious in Figures 5C and 5F, which depict the same homozygous retina labeled with both antibodies. Thus, not only is there a higher density of vessels in retinae that contain more astrocytes, but the distribution of vessels seems to be restricted by the extent of the astrocyte network. This emphasizes the interdependence of astrocytes and blood vessels during both normal and abnormal retinal development.

During early postnatal development, the NSE-PDGF-A retinae displayed retinal hemorrhage, especially in homozygous animals (data not shown). This might be a result of overproduction of vascular endothelial cell growth factor/vascular permeability factor (VEGF/VPF) by the excess astrocytes in these retinae. Retinal astrocytes have been shown to express VEGF/VPF in an oxygen-dependent manner during normal development (Shweiki et al., 1992; Stone et al., 1995).

Retinal Astrocytes in NSE-PDGF-A Mice Are More Numerous and Proliferate More than Normal

To confirm that the abnormal appearance of the astrocyte net in NSE-PDGF-A mice was due to increased

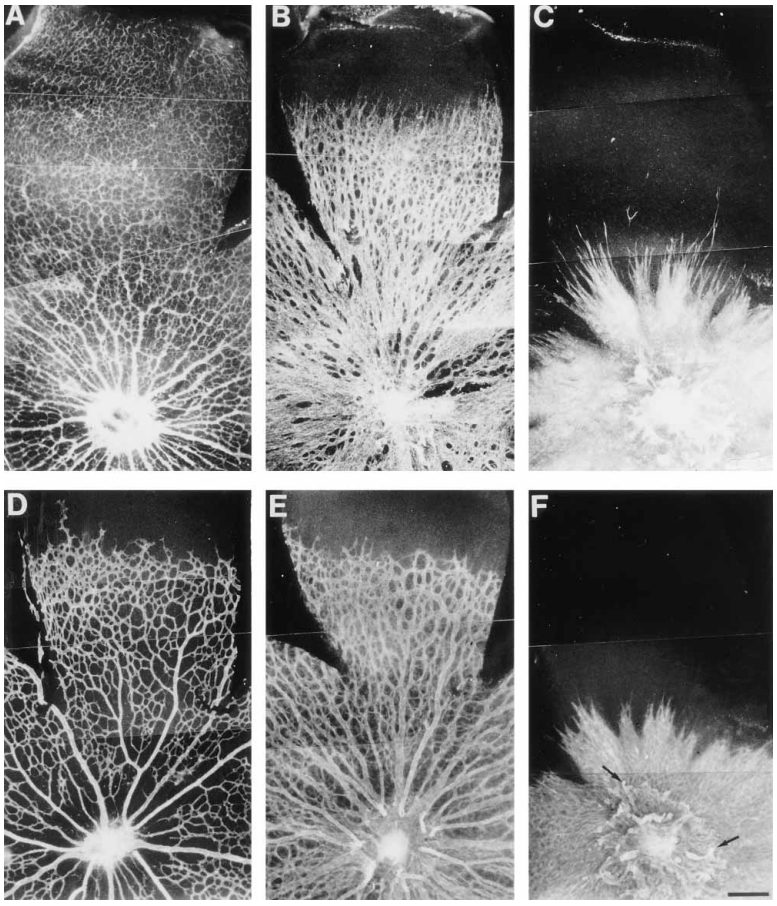

Figure 5. Hyperplasia, but Decreased Migration, of Retinal Astrocytes and Blood Vessels in NSE-PDGF-A Transgenic Mice

Retinal astrocytes (A–C) and inner vasculature (D–F) in P4 wild-type (A and D), hemizygous transgenic (B and E), and homozygous transgenic (C and F) littermates were visualized by anti-GFAP labeling (A–C) and anti-collagen IV labeling (D–F) of retinal whole-mounts. Only part of each preparation is shown, including the optic nerve head (bottom) and one lobe of the whole-mount. With increasing hPDGF-A transgene dose, the astrocyte network becomes more dense, and advances less far from the optic nerve head. The vasculature in the wild-type retina (D) forms an even network that does not yet extend all the way to the retinal periphery, even though astrocytes have already reached the periphery (compare with [A]). In the hemizygous transgenic animal (E), the retinal vessels form a denser network; there appear to be more and thicker vessels compared with wild-type. Note that the transgenic vascular net extends approximately to the leading edge of the astrocyte net, but does not overtake it (compare with [B]). In the homozygous transgenic retina (F), the vasculature forms a dense mat and extends a relatively short distance from the optic nerve head, closely corresponding to the distribution of astrocytes (compare with [C], which shows the same retina double-labeled for GFAP). Thus, the distribution of blood vessels in the transgenic retinae appears to be determined by the distribution of astrocytes. In (F), note vessels growing away from the retina into the vitreous (arrows). Scale bar, 200 μm.

numbers of astrocytes rather than, for example, more extensive GFAP$^+$ processes on the same number of cells, we enzymatically dissociated individual retinae from P3 and P6 wild-type and transgenic (A5-75) retinae and labeled them in suspension with anti-GFAP antibodies followed by FITC-conjugated second antibodies. The cells were also incubated with propidium iodide (PI) to label nuclear DNA and analyzed in a fluorescence-activated cell scanner (FACS). Representative primary FACS data for one wild-type and one hemizygous transgenic mouse are shown in Figures 6A and 6B, and combined data from several animals are plotted in Figures 6D and 6E (details in the figure legend). A control in which the primary antibody (anti-GFAP) was omitted is shown in Figure 6C. Cells with GFAP labeling greater than background (boxed regions in the FACS plots of Figures 6A–6C) were counted as a proportion of the total retinal cell population. There were more than twice the normal number of GFAP$^+$ astrocytes in the transgenic retinae at P3, and about four times the normal number at P6 (Figure 6D). In the transgenic retinae, there was also a higher proportion of astrocytes in the S, G2, and M phases of the cell cycle (15.6% $\pm$ 2.4% compared with 10.4% $\pm$ 1.0% in wild type, means $\pm$ SDs). This suggests that proliferation of astrocytes is enhanced in the transgenic retinae. We cannot yet say whether this effect accounts completely for the increased number of astrocytes in the transgenic retinae. For example, it is possible that increased survival of astrocytes also contributes to the phenotype.

Adult NSE-PDGF-A Mice Display a Phenotype Resembling Human Proliferative Retinopathy

In normal adult retinae, astrocytes are only found on the inner surface and never deep within the retina (Figure 7A). In adult transgenics, the astrocytes formed an abnormally tight mesh on the inner surface of the retina (data not shown) and, in addition, penetrated into the neural retina to form abnormal extensions of the net throughout the retina and even as deep as the retinal pigmented epithelium (Figure 7B).

In adult wild-type mice, blood vessels are limited to well defined planes at the inner surface of the retina and in the plexiform layers (arrows in Figure 7C), where they border the inner nuclear layer (Engerman and Meyer, 1965; Connolly, 1991). The outer vascular network develops during the second postnatal week by budding from the inner vasculature, and is independent of astrocytes (Engerman and Meyer, 1965; Stone et al., 1995). In adult hemizygous transgenics, blood vessels penetrated into all layers of the retina right out to the photoreceptor layer (arrows in Figure 7D). Confocal microscopy revealed that they were colocalized with GFAP$^+$ glial cells, most likely astrocytes (data not shown). The lamellar

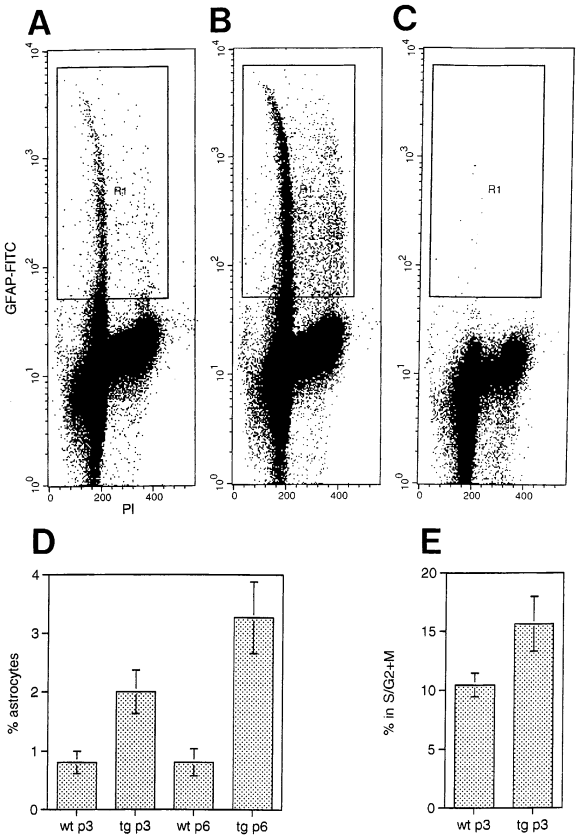

Figure 6. FACS Analysis of Astrocytes in Retinae of Wild-Type and Transgenic Littermates

(A–C) Primary data for dissociated P3 retinal cells sorted by anti-GFAP fluorescence intensity (ordinate) and propidium iodide (PI) fluorescence intensity (abscissa).

(A)–(C) Wild-type (A) and hemizygous transgenic (B and C) retinal cells. The anti-GFAP antibody was omitted in (C).

(D) Cells falling within the gate represented by the rectangular boxes in (A)–(C) (i.e., GFAP$^+$ astrocytes) were plotted as a proportion of the total number of retinal cells (mean and SDs of twelve wild-type and five transgenic animals from two P3 litters, twelve wild-type and three transgenic animals from two P6 litters). Since the total number of retinal cells did not change significantly in the transgenic animals (data not shown), there are approximately twice as many astrocytes as normal in the P3 transgenic retinae, and four times as many in the P6 transgenic retinae.

(E) Numbers of GFAP$^+$ astrocytes in the S/G2 and M phases of the cell cycle (PI fluorescence greater than 240 arbitrary units in [A]–[C]) were plotted as a proportion of the total number of astrocytes in each retina (means and SDs of six wild-type and three transgenic animals from one P3 litter). A greater proportion of astrocytes in the transgenic retinae is in S/G2+M compared with their wild-type littermates.

structure of the retina was disrupted in places, presumably a physical effect of the invading vasculature (large arrow, Figure 7D).

Discussion

The fact that PDGF-A and PDGFRα are expressed in the rodent retina by RGCs and astrocytes, respectively, suggests that PDGF-A might mediate a short-range paracrine interaction between these two cell types during normal development (Mudhar et al., 1993). The experiments reported here were designed to test whether such an interaction does occur and, if so, what the nature of the interaction might be. We attempted to inhibit PDGF signaling through PDGFRα on astrocytes, both with a blocking anti-PDGFRα antibody and also with a soluble extracellular fragment of PDGFRα. Both treatments resulted in significant but incomplete inhibition of astrocyte migration and a reduced branching pattern of the astrocyte network. Because we cannot tell to what extent PDGF signaling was inhibited in our experiments, we cannot deduce whether PDGF is wholly or only partly responsible for astrocyte proliferation/migration during development. It is possible that development of the astrocyte network depends solely on PDGF and that our inhibitory regimes were inadequate to reveal this. It is perhaps more likely that PDGF normally acts in concert with other factors whose individual contributions to astrocyte development are relatively small but whose combined effects are cumulative. If so, eliminating any one of them would not necessarily have a catastrophic effect.

To gain further information about the activity of PDGF-A in the retina, we generated transgenic mice that express PDGF-A under control of the NSE promoter. Although we were unable to visualize the transgene-derived secreted PDGF-A directly in situ, we showed, in two independent lines of transgenic mice, that an ER-retained form of PDGF-A under NSE control is expressed strongly in RGCs and less strongly in other retinal neurons. This is in accord with experience of other NSE-driven transgenes (Forss-Petter et al., 1990; Seiler and Aramant, 1995; Martinou et al., 1994), demonstrating that the activity of the NSE promoter cassette in the retina is robust, reproducible, and refractory to *cis*-acting effects of the transgene or neighboring chromosomal sequences. The ER-retained PDGF-A transgene did not elicit any retinal phenotype, unlike the secreted PDGF-A transgene, providing strong genetic evidence that the phenotype of our NSE-PDGF-A mice results from synthesis and secretion of the encoded PDGF-A polypeptide. Therefore, our transgenic mice demonstrate that increasing the supply of PDGF-A, most likely from RGCs (which also express endogenous PDGF-A), dramatically enhances accumulation of neighboring retinal astrocytes and their associated blood vessels. FACS analysis showed that the proportion of astrocytes containing more than a diploid complement of DNA is also increased. One possible interpretation of this observation is that the time the cells spend in G1 is reduced in proportion to the time spent in S/G2 and M, that is, the cell cycle is accelerated. Alternatively, the proportion of astrocytes that is actively engaged in the cell cycle might be increased in the transgenic mice. At present, we cannot distinguish between these possibilities. Nevertheless, we can conclude from the present data that PDGF-A overproduction in the transgenic mice has a positive effect on retinal astrocyte proliferation. It is possible that there is also an effect on astrocyte survival.

The fact that increased levels of PDGF-A stimulate

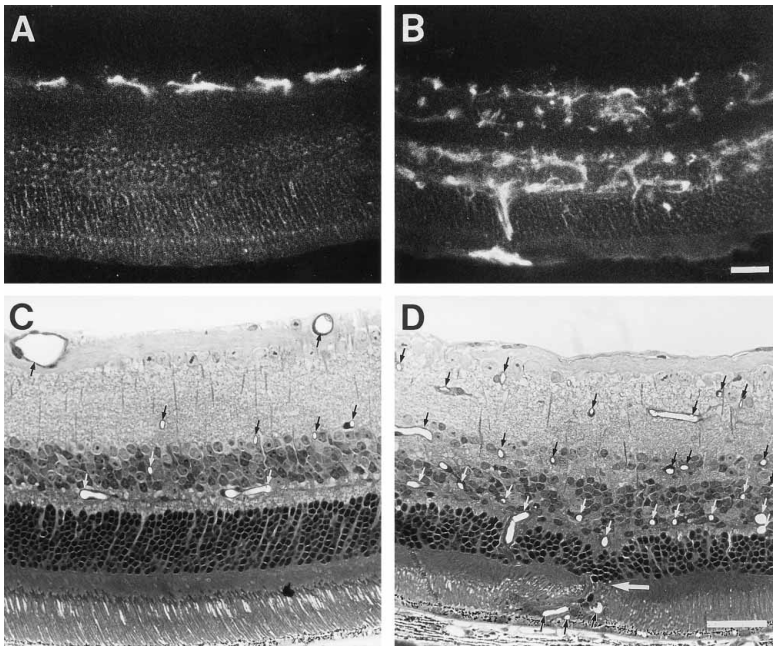

Figure 7. Retinae of Adult NSE-PDGF-A Transgenic Mice Have Similarities to Human Proliferative Retinopathies

Sections through adult wild-type (A and C) and hemizygous transgenic (B and D) retinae were immunolabeled with anti-GFAP to reveal the distribution of astrocytes (A and B) or stained with methylene blue and photographed in bright-field to show retinal morphology (C and D). Whereas astrocytes in the wild-type retina (A) are restricted to the inner surface (nerve fiber layer), astrocytes are distributed through all retinal layers right out to the pigment epithelium in the transgenic retina (B). This aberrant distribution of astrocytes is reflected by the vasculature in the transgenics. Whereas blood vessels in the wild-type retina are restricted to the nerve fiber layer and to the inner and outer faces of the inner nuclear layer (small arrows in [C]), they are more abundant and are distributed throughout the depth of the transgenic retina (small arrows in [D]). Presumably because of this vascular invasion of the retina, the normal lamellar organization of the retina is disrupted in places (e.g., large arrow in [D]). Scale bars, 50 μm.

astrocyte proliferation demonstrates that neither PDGF-A nor any other mitogenic factor is available in the normal developing mouse retina at a concentration that is saturating for astrocyte proliferation. It follows that the number of astrocytes that develop in the retina could potentially be determined by the rate of supply of PDGF-A, which in turn depends on the number of RGCs. It is known that the final number of RGCs, in common with many other neuronal populations, depends on survival signals from their target cells. It is also strongly suspected that the number of vascular cells that develop in the retina depends on astrocytes (see below), and the data presented here support this idea. Therefore, there appears to be a hierarchy of sequential cell–cell interactions among vascular cells, astrocytes, RGCs and their target cells, the purpose of which is to ensure that each cell population develops in proportion to the others. We suggest that PDGF-AA is an important link in this chain of number-matching interactions, acting as an RGC-derived mitogen for astrocytes and thereby controlling the proportion of astrocytes to RGCs.

An unexpected finding was that, despite the considerable increase in astrocyte numbers in the transgenics, migration away from the optic nerve head was retarded. Superficially, it might appear that stimulating and inhibiting PDGF signaling have similar effects on the astrocyte network but this is not so; inhibiting PDGF signaling with the Rα17 truncated receptor or APA5 anti-PDGFRα Ig resulted in a less extensive and more sparse astrocyte network, whereas increasing PDGF supply in the transgenics resulted in a less extensive but much denser network. PDGF-AA has been reported to either stimulate or inhibit cell migration, depending on its concentration and the cell type under investigation (Ferns et al., 1990; Siegbahn et al., 1990; Uren et al., 1994; Koyama et al., 1994a; Iguchi et al., 1995). For example, migration of Swiss 3T3 fibroblasts in vitro is maximal at relatively low PDGF-AA concentrations (3 ng/ml) and completely abolished at higher concentrations (12 ng/ml), whereas the proliferative response to PDGF-AA is monophasic and reaches a plateau at comparatively high concentrations (25 ng/ml) (Abedi et al., 1995). PDGF-AA has also been reported to antagonize PDGF-BB-stimulated cell migration (Siegbahn et al., 1990; Koyama et al., 1992). It seems likely that the signal transduction pathways that stimulate cell proliferation and migration interact but, in general, the relationship between proliferation and migration is poorly understood. An alternative explanation for the altered distribution of astrocytes in the transgenic retinae might be that this reflects an altered expression pattern of PDGF-A. We think that this is less likely, because the postnatal expression pattern of our ER-retained form of PDGF-A and other NSE-driven transgenes (Forss-Petter et al., 1990; Martinou et al., 1994; Seiler and Aramant, 1995) is rather similar to the expression pattern of endogeneous PDGF-A (Mudhar et al., 1993). Both transgene-derived and endogenous PDGF-A are expressed in the great majority of RGCs all the way from optic nerve head to the retinal periphery, and in other retinal neurons in the inner and outer nuclear layers.

A striking aspect of the transgenic phenotype was the close correspondence between the distribution patterns of retinal astrocytes and blood vessels. In wild-type mice, the astrocytes migrate from the optic nerve head slightly ahead of the developing vascular network. In transgenic retinae, where astrocyte migration was retarded, the leading edge of the blood vessels caught up with but did not overtake the astrocyte front. This was true even in homozygous transgenic retinae, where astrocyte migration was severely inhibited. This is consistent with the view that physical proximity of astrocytes is required for retinal vasculogenesis. Retinal astrocytes express PDGFRα and probably respond directly to the transgene-encoded hPDGF-A. However, vascular cells express PDGFRβ (Mudhar et al., 1993)

and would not be expected to respond directly to PDGF-AA (Heldin et al., 1988; Coats et al., 1994). In keeping with this expectation, neither pericytes nor endothelial cells respond to PDGF-AA in vitro (D'Amore and Smith, 1993). Therefore, vascular cells in the transgenic retinae are probably stimulated by secondary signals from the PDGF-AA-responsive astrocytes. A strong candidate for an astrocyte-derived vasculogenic factor is VEGF/VPF (Barinaga, 1995). This factor is synthesized by retinal astrocytes in vivo (Stone et al., 1995), and is regulated by oxygen tension both in vivo and in vitro. Thus, experimentally induced hypoxia results in up-regulation of VEGF mRNA and stimulates vasculogenesis (Shweiki et al., 1992; Alon et al., 1995; Pierce et al., 1995; Stavri et al., 1995; Stone et al., 1995), whereas hyperoxia has the reverse effect (Alon et al., 1995). We did not investigate VEGF expression in our transgenic mice, but the fact that the overextended retinal vasculature was leaky and released blood into the retina is consistent with the known activities of VEGF/VPF (Connolly, 1991).

In adult NSE-PDGF-A transgenic retinae, astrocytes were distributed throughout the depth of the retina, including the inner and outer plexiform layers and as far out as the retinal pigment epithelium. This is in striking contrast to wild-type retinae, in which astrocytes are found only at the inner retinal surface (Stone et al., 1995). It seems likely that this is a consequence of overexpression of the NSE-PDGF-A transgene in neurons of the inner and outer nuclear layers (Forss-Petter et al., 1990; Figure 4C), although it is unclear how the effect is elicited. For example, PDGF-A overexpression might trigger abnormal outward migration of astrocytes into the retina, or it might allow inappropriate survival of astrocytes that might normally migrate outward but that usually die for lack of survival signals. It is likely that these inappropriately located astrocytes are responsible for inducing the excessive and misplaced vascularization that is observed throughout the depth of the adult transgenic retina.

Inappropriate vascularization of the retina is the hallmark of proliferative retinal diseases, such as proliferative diabetic retinopathy (PDR) or age-related macular degeneration; in each of these human disorders, inappropriate neovascularization of the retina can lead to blindness (D'Amore, 1994; Barinaga, 1995). VEGF is now thought to play a key role in ischemia-associated retinopathies such as PDR and retinopathy of prematurity (Aiello et al., 1994; D'Amore, 1994; Alon et al., 1995; Barinaga, 1995; Pe'er et al., 1995). Retinal astrocytes are known to produce VEGF (see above) and are thought to participate in the pathogenesis of human retinopathies (Jerdan et al., 1986; Sramek et al., 1989; Ohira and de Juan, 1990; Hosada et al., 1993; Alon et al., 1995). Thus, factors that influence astrocytes (such as PDGF-AA) might be expected to deregulate VEGF production, resulting in neovascularization. PDGF and PDGF receptors have previously been implicated in the pathogenesis of human proliferative retinopathies (Robbins et al., 1994). Human serum levels of PDGF (50–70 ng/ml) are high enough that, following intraocular hemorrhage, the retina might be exposed to concentrations of PDGF that would be sufficient to reinitiate astrocyte proliferation and subsequent neovascularization (Uchihori and Puro, 1991). Therefore, our transgenic mice might model a naturally occurring human disease state and could prove useful for testing potential treatments for some aspects of the proliferative retinopathies.

Experimental Procedures

Construction of pRα17 Plasmid Expression Vector

A full-length cDNA encoding rat PDGFRα (Lee et al., 1990) was obtained from R. Reed (John Hopkins, Baltimore). A 1.7 kb fragment of this cDNA was obtained following digestion with EcoRI and NotI, and inserted into a COS cell expression vector based on pHYK (Pollock and Richardson, 1992), which contains the adenovirus major late promoter, polyadenylation site from the herpesvirus type-1 thymidine kinase gene, and simian virus 40 origin of replication. This vector can replicate autonomously in COS cells under the influence of the endogenous SV40 large-T antigen. The PDGFRα insert includes a small amount of 5′ noncoding sequence, followed by the initiation codon and coding sequence up to, but not including, the transmembrane domain. The mode of construction also placed a c-Myc epitope tag in-frame at the extreme carboxy terminus of the encoded receptor fragment, so that it could be recognized by monoclonal antibody 9E10 (Evan et al., 1985). The final construct was named pRα17, and the encoded polypeptide Rα17.

Electroporation of COS Cells

DNA-encoding truncated rat PDGFRα (Rα17) or a similar plasmid encoding the short splice-variant of human PDGF-A (Pollock and Richardson, 1992) was introduced into cultured COS cells by electroporation. The cells were grown to about 70% confluence in Dulbecco's modified Eagle's medium (DMEM) containing 10% fetal calf serum (FCS), trypsinized, and washed twice in HBS (20 mM Hepes [pH 7.05], 137 mM NaCl, 5 mM KCl, 0.7 mM Na_2HPO_4, 6 mM D-glucose), and resuspended in HBS at a concentration of 8×10^6 cells/ml. We mixed 2×10^6 cells with 15 μg of DNA and electroporated with a Biorad apparatus at 320 V and 125 μF, giving a time constant of 4.9 μs. After electroporation, the cells were grown in DMEM containing 10% FCS for 48 hr on plastic tissue culture dishes prior to intravitreal injection (see below) or on glass coverslips for immunocytochemistry with anti-c-Myc monoclonal antibody 9E10.

Metabolic Radiolabeling of COS Cells

About 5×10^5 electroporated COS cells were plated into 25 cm^2 tissue culture dishes and grown for 48 hr before washing once with phosphate-buffered saline (PBS). The culture medium was replaced with cysteine- and methionine-free DMEM containing 10% dialysed fetal calf serum (FCS) and 60 μCi/ml ^{35}S-cysteine/methionine mixture (Translabel, Amersham). After 16 hr incubation, the cell supernatant was centrifuged at 25,000 × g for 20 min and stored at 4°C before use.

Immunoprecipitation and Gel Electrophoresis

^{35}S-labeled supernatants from COS cells expressing truncated rat PDGFRα, or human PDGF-A, were preincubated with 10^{-3} volume of normal mouse serum for 1 hr at 4°C, then with protein A-Sepharose for 1 hr, followed by centrifugation at 15,000 × g for 10 min. The Rα17 supernatant was then incubated with an equal volume of either DMEM or PDGF-A supernatant for 16 hr at 4°C. The supernatants were immunoprecipitated with either mouse monoclonal antibody 9E10 or rabbit antiserum raised against PDGF from human platelets (R and D Systems, Minneapolis). After precipitation of immune complexes with protein A-Sepharose, they were electrophoresed on a 10% nonreducing polyacrylamide gel containing SDS and visualized by fluorography (Bonner and Laskey, 1974).

^{3}H-Thymidine Incorporation Assays

Approximately 2×10^4 NIH 3T3 cells were plated in each well of a 24-well tissue culture plate and cultured overnight in DMEM containing 10% FCS. After two washes with DMEM, the cells were growth-arrested by incubation in DMEM containing 0.25% FCS for 30 hr. DMEM-containing recombinant PDGF homodimers or bFGF

(all human sequence, from Peprotech, New York), or PDGF-AB purified by metal ion chromatography from human platelets (Hammacher et al., 1988; a generous gift from Carl-Henrik Heldin), with or without medium conditioned by COS cells expressing Rα17, was added to the cells, which were cultured for a further 16 hr at 37°C before the addition of 1–3 μCi of ^{3}H-thymidine. The concentrations of growth factors used were sufficient to exert a half-maximal effect on ^{3}H-thymidine incorporation in the absence of any conditioned medium: 2 ng/ml for PDGF-AA and PDGF-AB, and 0.5 ng/ml for PDGF-BB and bFGF. After 4 hr incubation in the presence of ^{3}H-thymidine, the medium was removed and the cells lysed and washed in situ three times with ice-cold 5% (w/v) trichloracetic acid (TCA). The precipitates remaining attached to the plastic were solubilized in 0.5 M NaOH, 1% (w/v) sodium dodecyl sulfate (SDS). The incorporated radioactivity was estimated by scintillation counting in Aquasol (Dupont).

Intravitreal Injection of COS Cells

For injection into the eyes of newborn rats, COS cells were cultured for 48 hr after electroporation, trypsinized and washed, and resuspended in HEPES MEM at a concentration of $\sim 2 \times 10^6$ cells/ml. In parallel, COS cells on coverslips from the same electroporation experiment were subjected to immunofluorescence microscopy with antibody 9E10 to monitor expression levels. COS cells were not used for intravitreal injection unless the proportion expressing Rα17 was greater than 15%. Approximately 10^3 cells (0.5 μl) were injected into the posterior chamber of one eye of newborn rat pups. The neonates were anesthetized with Metofane (C-Vet Ltd., Bury St. Edmunds), and the eyelids eased apart using a pair of microscissors under a dissecting microscope. Using a Hamilton syringe with a 34 gauge needle, the cells were injected over a period of 2 min. After completion of the injection, the needle was left in position for 30 s to reduce reflux of the injected cells. Control injections of mock-electroporated COS cells, or the vehicle alone, were always conducted on rats from the same litter.

Histology and Immunocytochemistry

For whole-mount preparations, eyes were removed and given a brief fixation in 4% (w/v) paraformaldehyde in phosphate-buffered saline (PBS). The retinae were subsequently dissected and fixed in ice-cold methanol. After incubating in PBS containing 50% fetal calf serum (FCS) and 1% (w/v) Triton X-100 for 30 min at room temperature, the retinae were incubated overnight at room temperature in primary antibody, washed for 1 hr in PBS, incubated for 3 hr at room temperature in fluorescent secondary antibody, washed for 1 hr, and mounted in Citifluor anti-fade reagent (City University, London). All antibodies were diluted in PBS containing 10% FCS. For cryosections, eyes were removed and fixed in 4% (w/v) paraformaldehyde in PBS for 1 hr and cryoprotected in 30% (w/v) solution of sucrose in PBS. Retinae were dissected in PBS, embedded in OCT (Raymond A. Lamp, London), and frozen in isopentane cooled by liquid nitrogen. Cryosections (12 μm nominal thickness) were prepared and stained as previously described (Mudhar et al., 1993). For semithin sections, deeply anaesthetized animals were perfused with cacodylate buffer (0.1 M [pH 7.4]) containing 4% (w/v) paraformaldehyde and 2% (w/v) glutaraldehyde. Retinae were dissected, fixed in cacodylate buffer containing 2% (w/v) OsO_4, dehydrated in ethanol, and embedded in TAAB resin (TAAB Laboratories Equipment Ltd., England). Semithin sections (1 μm nominal thickness) were stained with methylene blue, 0.2% (w/v) in water.

Antibodies

For whole-mount preparations, a mouse monoclonal antibody raised against pig glial fibrillary acidic protein (GFAP) (Sigma Immuno Chemicals) and a polyclonal rabbit antibody raised against murine collagen IV (Biogenesis, England) were used as primary antibodies. A polyclonal rabbit anti-GFAP antibody (Pruss, 1979) was used in flow cytometry. The latter anti-GFAP antibody and monoclonal antibody 9E10 (Evan et al., 1985) were used for immunohistochemistry on cryosections. The monoclonal antibody (IgG 2a) against PDGFRα (clone APA5) was raised against recombinant mouse PDGFRα in rat and competes with PDGF for binding to PDGFRα in vitro (Takakura et al., 1996). Hybridoma culture-supernatants were precipitated with saturated amonium sulfate at 50% (v/v) concentration. The precipitate was further purified by anion-exchange chromatography (Clezardin et al., 1985). A monoclonal rat antibody (IgG 2a) against mouse c-Kit (clone ACK2; Nishikawa et al., 1991) was used as a negative control for the effects of APA5. Fluorescein isothiocyanate (FITC)-conjugated anti-mouse antibodies, FITC-conjugated anti-rat antibodies, FITC-conjugated anti-rabbit antibodies, and tetramethyl rhodamine isothiocyanate (TRITC)-conjugated anti-rabbit antibodies (Sigma Immuno Chemicals) were used as secondary antibodies.

Production of Transgenic Mice

Mice that overexpress PDGF-A in neurons under control of the NSE gene promoter were generated at the UMDS Transgenic Unit, The Rayne Institute, St. Thomas's Hospital, London SEI 7EH. The transgene consisted of a partial human PDGF-A cDNA (Betsholtz et al., 1986) engineered to encode the "short" alternative splice PDGF-A isoform (Tong et al., 1987; Bonthron et al., 1988; Rorsman et al., 1988) with a Myc epitope tag (Evan et al., 1985) at its carboxy terminus, fused to the rat NSE promoter (Forss-Petter et al., 1990) and the SV40 early polyadenylation site (Figure 4A). In brief, the SacII site upstream of the initiation codon in plasmid "PDGF-A_S+TAG" (Pollock and Richardson, 1992) was converted to a HindIII site by T4 bacteriophage DNA polymerase treatment and addition of a HindIII linker, then a HindIII–EcoRI fragment containing the complete human PDGF-A coding sequence with Myc tag attached and part of the PDGF-A mRNA 3′ untranslated region was excised and used to replace the *lacZ* fusion gene in plasmid "NSElacZ" (Forss-Petter et al., 1990), leaving the SV40 poly(A)-addition site intact. This placed human PDGF-A under the control of 1.8 kb of rat NSE promoter sequences and the SV40 early poladenylation site. The entire NSE-PDGF-SV40 cassette was purified as a linear EcoRI fragment for injection into mouse oocytes (C57Bl/6 × CBA f1 hybrids).

Identification and Genotyping of Transgenic Animals

Tail clippings were digested overnight at 55°C in a buffer containing 50 mM Tris (pH 8), 10 mM EDTA, 100 mM sodium chloride, 1% (w/v) SDS, and 50 mg/ml proteinase K (Sigma). Following RNase A treatment (100 μg/ml, 1 hr at 37°C), ammonium acetate was added to a final concentration of 2 M, chilled on ice, and centrifuged to precipitate proteins. DNA in the supernatant was precipitated with 0.6 vol of cold isopropanol and washed with 70% ethanol. The DNA pellet was dissolved in water overnight at 4°C. Yields were estimated from absorbance at 260 nm, and DNA aliquots (10 μg) were digested with restriction enzymes and subjected to Southern blot analysis. The blots were hybridized with a PDGF-A chain cDNA probe radiolabeled by random priming (Feinberg and Vogelstein, 1984).

RT–PCR

Retinae were dissected from wild-type and transgenic littermates and homogenized in guanidinium isothiocyanate, and total cellular RNA was prepared as described previously (Chomczynski and Sacchi, 1987). This was treated with 400 units/ml RNase-free DNase 1 (Pharmacia) for 15 min at 37°C, then phenol/chloroform-extracted and precipitated with ethanol. Total RNA (2 μg) was reverse-transcribed into cDNA using the Superscript preamplification system (Gibco-BRL). PDGF-A sequences were then specifically amplified by PCR (25 cycles of the following): 94°C, 30 s; 55°C, 2 min; 72°C, 2 min; concluding with 72°C, 10 min). The PCR primers were as follows: 5′-GTCCAGGTGAGGTTAGAGGA-3′ (upstream) and 5′-TCA CGGAGGAGAACAAAGAC-3′ (downstream). These hybridized to both endogenous (mouse) and transgenic (human) PDGF-A sequences without mismatch. RNA titration experiments showed that the RT–PCR reaction was semiquantitative under these conditions (i.e., operating in the linear range). The PCR products were separated on a 2% (w/v) agarose gel, which was Southern blotted onto nylon membrane (Zetaprobe, BioRad) and probed with ^{32}P-labeled (using polynucleotide kinase) oligonucleotide probes against either PDGF-A or the Myc epitope tag (see Figure 4). The oligonucleotide probe against PDGF-A was an equimolar mixture of two 39-mers, 5′-AAGCACC**A**TACATAGT**A**T**G**TTCAGGAATGT**C**A CACGCCA-3′ (mouse) and 5′-AAGCACC**G**TACATAGT**AG**GTTCAGG

AATGTAACACGCCA-3′ (human). The probe for Myc sequences was a 44-mer oligonucleotide, 5′-CCTGAGCAAAAGCTCATTTCTGAAG AGGACTTGCTCGAGTA GCC-3′. The blots were exposed and scanned using a BioRad GS-250 Molecular Imager with a BI screen to quantitate band intensities.

Flow Cytometry

Retinae were dissected and collected in Mg^{2+}/Ca^{2+}-free Earl's basal salt solution (EBSS; Gibco) and incubated for 1 hr at 37°C in 0.125% (w/v) trypsin (Sigma) in EBSS followed by 30 min at 37°C in 0.125% (w/v) type I collagenase (Sigma) in DMEM. Cells were mechanically dissociated by trituration through a yellow Eppendorf tip in PBS containing 20% FCS, 6 mM $MgCl_2$, and 50 mg/ml DNase I (Sigma). The cells were fixed for 30 min in 70% ethanol on ice and labeled with rabbit anti-GFAP and FITC-conjugated anti-rabbit antibodies in PBS containing 10% FCS. To analyze DNA content, 1 mg/ml RNase A was present during the first antibody incubation (anti-GFAP) and 25 μg/ml propidium iodide (PI; Sigma) during the second (anti-rabbit). Cells were analyzed by flow cytometry in a fluorescence-activated cell scanner (FACS) (Becton-Dickinson) to quantitate GFAP-immunoreactivity and cellular DNA content.

Acknowledgments

We would like to thank the other members of our respective laboratories for ideas, advice, and practical help. We would particularly like to thank Derek Davis for help with FACS, Frank Grosveld for help and advice on transgenics, Frank Walsh and Alex Harper (UMDS Transgenic Unit, St. Thomas's Hospital, London SEI 7EH) for transgenic mouse production. This research was supported by the UK Medical Research Council, the Multiple Sclerosis Society of Great Britain and Northern Ireland, and a Wellcome Prize studentship to H. S. M.; M. F. is the recipient of a Royal Society/Swiss National Research Foundation exchange fellowship.

The costs of publication of this article were defrayed in part by the payment of page charges. This article must therefore be hereby marked *"advertisement"* in accordance with 18 USC Section 1734 solely to indicate this fact.

Received July 22, 1996; revised October 16, 1996.

References

Abedi, H., Dawes, K.E., and Zachary, I. (1995). Differential effects of platelet-derived growth factor BB on p125 focal adhesion kinase and paxillin tyrosine phosphorylation and on cell migration in rabbit aortic vascular smooth muscle cells and Swiss 3T3 fibroblasts. J. Biol. Chem. *270*, 11367–11376.

Aiello, L.P., Avery, R.L., Arrigg, P.G., Keyt, B.A., Jampel, H.D., Shah, S.T., Pasquale, L.R., Thieme, H., Iwamota, M.A., and Park, J.E.e.a. (1994). Vascular endothelial growth factor in ocular fluid of patients with diabetic retinopathy and other retinal disorders. N. Engl. J. Med. *331*, 1480–1487.

Alon, T., Hemo, I., Itin, A., Pe'er, J., Stone, J., and Keshet, E. (1995). Vascular endothelial growth factor acts as a survival factor for newly formed retinal vessels and has implications for retinopathy of prematurity. Nature Med. *1*, 1024–1028.

Barinaga, M. (1995). Shedding light on blindness. Science *267*, 452–453.

Betsholtz, C., Johnsson, A., Heldin, C.-H., Westermark, B., Lind, P., Urdea, M.S., Eddy, R., Shows, T.B., Philpott, K., Mellor, A.L., Knott, T.J., and Scott, J. (1986). cDNA sequence and chromosomal localization of human platelet-derived growth factor A-chain and its expression in human tumour cell lines. Nature *320*, 695–699.

Bonner, W.M., and Laskey, R.A. (1974). A film detection method for tritium-labelled proteins and nucleic acids in polyacrylamide gels. Eur. J. Biochem. *46*, 83–88.

Bonthron, D.T., Morton, C.C., Orkin, S.H., and Collins, T. (1988). Platelet-derived growth factor A chain: gene structure, chromosomal location and basis for alternative splicing. Proc. Natl. Acad. Sci. USA *85*, 1492–1496.

Breitman, M.L., Bryce, D.M., Giddens, E., Clapoff, S., Goring, D., Tsui, L.-C., Klintworth, G.K., and Bernstein, A. (1989). Analysis of lens fate and eye morphogenesis in transgenic mice ablated for cells of the lens lineage. Development *106*, 457–463.

Chang-Ling, T. (1994). Glial, neuronal and vascular interactions in the mammalian retina. Prog. Retinal Res. *13*, 357–389.

Chomczynski, P., and Sacchi, N. (1987). Single-step method of RNA isolation by acid guanidinium thiocyanate-phenol-chloroform extraction. Anal. Biochem. *162*, 156–159.

Clezardin, P., McGregor, J.L., Manach, M., Boukerche, H., and Dechavanne, M. (1985). One-step procedure for the rapid isolation of mouse monoclonal antibodies and their antigen binding fragments by fast protein liquid chromatography on a mono Q anion-exchange column. J. Chromatogr. *319*, 67–77.

Coats, S.R., Love, H.D., and Pledger, W.J. (1994). Platelet-derived growth factor (PDGF)-AB-mediated phosphorylation of PDGF beta receptors. Biochem. J. *297*, 379–384.

Connolly, D.T. (1991). Vascular permeability factor: a unique regulator of blood vessel function. J. Cell. Biochem. *47*, 219–223.

D'Amore, P.A. (1994). Mechanisms of retinal and choroidal neovascularization. Invest. Ophthalmol. Vis. Sci. *35*, 3974–3979.

D'Amore, P.A., and Smith, S.R. (1993). Growth factor effects on cells of the vascular wall: a survey. Growth Factors *8*, 61–75.

Engerman, R.L., and Meyer, R.K. (1965). Development of retinal vasculature in rats. Am. J. Ophthalmol. *60*, 628–641.

Evan, G.I., Lewis, G.K., Ramsay, G., and Bishop, J.M. (1985). Isolation of monoclonal antibodies specific for human c-myc proto-oncogene product. Mol. Cell. Biol. *5*, 3610–3616.

Feinberg, A.P., and Vogelstein, B. (1984). A technique for radiolabelling DNA restriction endonuclease fragments to high specific activity. Anal. Biochem. *173*, 266–267.

Ferns, G.A., Sprugel, K.H., Seifert, R.A., Bowen-Pope, D.F., Kelly, J.D., Murray, M., Raines, E.W., and Ross, R. (1990). Relative platelet-derived growth factor receptor subunit expression determines cell migration to different dimeric forms of PDGF. Growth Factors *3*, 315–324.

Forss-Petter, S., Danielson, P.E., Catsicas, S., Battenberg, E., Price, J., Nerenberg, M., and Sutcliffe, J.G. (1990). Transgenic mice expressing (-galactosidase in mature neurons under neuron-specific enolase promoter control. Neuron *5*, 187–197.

Gronwald, R.G.K., Grant, F.J., Haldeman, B.A., Hart, C.E., O'Hara, P.J., Hagen, F.S., Ross, R., Bowen-Pope, D.F., and Murray, M.J. (1988). Cloning and expression of a cDNA coding for the human platelet-derived growth factor receptor: evidence for more than one receptor class. Proc. Natl. Acad. Sci. USA *85*, 3435–3439.

Hammacher, A., Hellman, U., Johnsson, A., Östman, A., Gunnarsson, K., Westermark, B., Wasteson, Å., and Heldin, C.-H. (1988). A major part of platelet-derived growth factor purified from human platelets is a heterodimer of one A and one B chain. J. Biol. Chem. *263*, 16493–16498.

Hart, C.E., Forstrom, J.W., Kelly, J.D., Seifert, R.A., Smith, R.A., Ross, R., Murray, M.J., and Bowen-Pope, D.F. (1988). Two classes of PDGF receptor recognize different isoforms of PDGF. Science *240*, 1529–1531.

Heldin, C.-H., and Westermark, B. (1989). Platelet-derived growth factor: three isoforms and two receptor types. Trends Genet. *5*, 108–111.

Heldin, C.H., Bäckström, G., Östman, A., Hammacher, A., Rönnstrand, L., Rubin, K., Nistér, M., and Westermark, B. (1988). Binding of different dimeric forms of PDGF to human fibroblasts: evidence for two separate receptor types. EMBO J. *7*, 1387–1393.

Herken, R., Gotz, W., and Thies, M. (1990). Appearance of laminin, heparan sulphate proteoglycan and collagen type IV during initial stages of vascularisation of the neuroepithelium of the mouse embryo. J. Anat. *169*, 189–195.

Holt, C.E., Bertsch, T.W., Ellis, H.M., and Harris, W.A. (1988). Cellular determination in the Xenopus retina is independent of lineage and birth date. Neuron *1*, 15–26.

Hosada, Y., Okada, M., Matsumura, M., Ogino, N., Honda, Y., and Nagai, Y. (1993). Epiretinal membrane of proliferative diabetic retinopathy: an immunohistochemical study. Ophthalmic Res. *25*, 289–294.

Iguchi, I., Kamiyama, K., Wang, X., Kita, M., Imanishi, J., Yamaguchi, N., Sotozono, C., and Kinoshita, S. (1995). Enhancing effect of platelet-derived growth factors on migration of corneal endothelial cells. Cornea *14*, 365–371.

Jerdan, J.A., Michels, R.G., and Glaser, B.M. (1986). Diabetic preretinal membranes: an immunohistochemical study. Arch. Ophthalmol. *104*, 286–290.

Kaur, S., Key, B., Stock, J., McNeish, J.D., Akeson, R., and Potter, S.S. (1989). Targeted ablation of (-crystallin-synthesising cells produces lens-deficient eyes in transgenic mice. Development *105*, 613–619.

Khachigian, L.M., Owensby, D.A., and Chesterman, C.N. (1992). A tyrosinated peptide representing the alternatively spliced exon of the platelet-derived growth factor A-chain binds specifically to cultured cells and interferes with binding of several growth factors. J. Biol. Chem. *267*, 1660–1666.

Klagsbrun, M., and Soker, S. (1993). VEGF/VPF: the angiogenesis factor found? Curr. Biol. *3*, 699–702.

Koyama, N., Morisaki, N., Saito, Y., and Yoshida, S. (1992). Regulatory effects of platelet-derived growth factor-AA homodimer on migration of vascular smooth muscle cells. J. Biol. Chem. *267*, 22806–22812.

Koyama, N., Hart, C.E., and Clowes, A.W. (1994a). Different functions of the platelet-derived growth factor-alpha and -beta receptors for the migration and proliferation of cultured baboon smooth muscle cells. Circ. Res. *75*, 682–691.

Koyama, N., Watanabe, S., Tezuka, M., Morisaki, N., Saito, Y., and Yoshida, S. (1994b). Migratory and proliferative effect of platelet-derived growth factor in rabbit retinal endothelial cells: evidence of an autocrine pathway of platelet-derived growth factor. J. Cell. Physiol. *158*, 1–6.

Landel, C.P., Zhao, J., Bok, D., and Evans, G.A. (1988). Lens-specific expression of recombinant ricin induces developmental defects in the eyes of transgenic mice. Genes Dev. *2*, 1168–1178.

LaRochelle, W.J., May-Siroff, M., Robbins, K.C., and Aaronson, S.A. (1991). A novel mechanism regulating growth factor association with the cell surface: identification of a PDGF retention domain. Genes Dev. *5*, 1191–1199.

Laterra, J., Guerin, C., and Goldstein, G.W. (1990). Astrocytes induce neural microvascular endothelial cells to form capillary-like structures in vitro. J. Cell. Physiol. *144*, 204–215.

Lee, K.-H., Bowen-Pope, D.F., and Reed, R.R. (1990). Isolation and characterization of the platelet-derived growth factor receptor from olfactory epithelium. Mol. Cell. Biol. *10*, 2237–2246.

Leung, D.W., Cachianes, G., Kuang, W.J., Goeddel, D.V., and Ferrera, N. (1989). Vascular endothelial growth factor is a secreted angiogenic mitogen. Science *246*, 1306–1309.

Ling, T., and Stone, J. (1988). The development of astrocytes in the cat retina: evidence of migration from the optic nerve. Brain Res. Dev. Brain Res. *44*, 73–85.

Ling, T., Mitrofanis, J., and Stone, J. (1989). Origin of retinal astrocytes in the rat: evidence of migration from the optic nerve. J. Comp. Neurol. *286*, 345–352.

Martinou, J.C., Dubois-Dauphin, M., Staple, J.K., Rodriguez, I., Frankowski, H., Missotten, M., Albertini, P., Talabot, D., Catsicas, S., Pietra, C., and Huarte, J. (1994). Overexpression of BCL-2 in transgenic mice protects neurons from naturally-occurring cell death and experimental ischemia. Neuron *13*, 1017–1030.

Millauer, B., Wizigmann-Voos, S., Schnurch, H., Martinez, R., Moller, N.P., Risau, W., and Ullrich, A. (1993). High-affinity VEGF binding and developmental expression suggest Flk-1 as a major regulator of vasculogenesis and angiogenesis. Cell *72*, 835–846.

Mudhar, H.S., Pollock, R.A., Wang, C., Stiles, C.D., and Richardson, W.D. (1993). PDGF and its receptors in the developing rodent retina and optic nerve. Development *118*, 539–552.

Nishikawa, S., Kuskabe, M., Yoshinaga, K., Ogawa, M., Hayashi, S., Kunisada, T., Era, T., Sakakura, T., and Nishikawa, S. (1991). In *utero* manipulation of coat color formation by a monoclonal anti-*c-kit* antibody: two distinct waves of *c-kit*-dependency during melanocyte development. EMBO J. *10*, 2111–2118.

Ohira, A., and de Juan, E.J. (1990). Characterization of glial involvement in proliferative diabetic retinopathy. Ophthalmol. *201*, 187–195.

Östman, A., Andersson, M., Betsholtz, C., Westermark, B., and Heldin, C.-H. (1991). Identification of a cell-retention signal in the B-chain of platelet-derived growth factor and in the long splice version of the A-chain. Cell Regul. *2*, 503–512.

Pe'er, J., Shweiki, D., Itin, A., Hemo, I., Gnessin, H., and Keshet, E. (1995). Hypoxia-induced expression of vascular endothelial growth factor by retinal cells is a common factor in neovascularizing ocular diseases. Lab. Invest. *72*, 638–645.

Peters, K.G., De Vriews, C., and Williams, L.T. (1993). Vascular endothelial growth factor expression during embryogenesis and tissue repair suggests a role in endothelial differentiation and blood vessel growth. Proc. Natl. Acad. Sci. USA *90*, 8915–8919.

Pierce, E.A., Avery, R.L., Foley, E.D., Aiello, L.P., and Smith, L.E. (1995). Vascular endothelial growth factor/vascular permeability factor expression in a mouse model of retinal neovascularization. Proc. Natl. Acad. Sci. USA *92*, 905–909.

Pollock, R.A., and Richardson, W.D. (1992). Alternative splicing generates two isoforms of the PDGF A-chain that differ in their ability to associate with the extracellular matrix and to bind heparin in vitro. Growth Factors *7*, 267–279.

Pruss, R. (1979). Thy-1 antigen on astrocytes in long-term cultures of rat central nervous system. Nature *303*, 396–399.

Raines, E.W., and Ross, R. (1992). Compartmentalization of PDGF on extracellular binding sites dependent on exon-6-encoded sequences. J. Cell Biol. *116*, 533–543.

Raymond, S.M., and Jackson, I.J. (1995). The retinal pigmented epithelium is required for development and maintenance of the mouse neural retina. Curr. Biol. *5*, 1286–1295.

Robbins, S.G., Mixon, R.N., Wilson, D.J., Hart, C.E., Robertson, J.E., Westra, I., Planck, S.R., and Rosenbaum, J.T. (1994). Platelet-derived growth factor ligands and receptors immunolocalized in proliferative retinal diseases. Invest. Ophthalmol. Vis. Sci. *35*, 3649–3663.

Rorsman, F., Bywater, M., Knott, T.J., Scott, J., and Betsholtz, C. (1988). Structural characterization of the human platelet-derived growth factor A-chain cDNA and gene: alternative exon usage predicts two different precursor proteins. Mol. Cell. Biol. *8*, 571–577.

Seiler, M.J., and Aramant, R.B. (1995). Transplantation of embryonic retinal donor cells labelled with BrdU or carrying a genetic marker to adult retina. Exp. Brain Res. *105*, 59–66.

Shweiki, D., Itin, A., Soffer, D., and Keshet, E. (1992). Vascular endothelial growth factor induced by hypoxia may mediate hypoxia-initiated angiogenesis. Nature *359*, 843–845.

Siegbahn, A., Hammacher, A., Westermark, B., and Heldin, C.-H. (1990). Differential effects of the various isoforms of platelet-derived growth factor on chemotaxis of fibroblasts, monocytes and granulocytes. J. Clin. Invest. *85*, 916–920.

Smits, A., Hermansson, M., Nistér, M., Karnushina, I., Heldin, C.-H., Westermark, F., and Funa, K. (1989). Rat brain capillary endothelial cells express functional PDGF B-type receptors. Growth Factors *2*, 1–8.

Sramek, S.J., Wallow, I.H., Stevens, T.S., and Nork, T.M. (1989). Immunostaining of preretinal membranes for actin, fibronectin, and glial fibrillary acidic protein. Ophthalmology *96*, 835–841.

Stavri, G.T., Hong, Y., Zachary, I.C., Breier, G., Baskerville, P.A., Yla-Herttuala, S., Risau, W., Martin, J.F., and Erusalimsky, J.D. (1995). Hypoxia and platelet-derived growth factor-BB synergistically upregulate the expression of vascular endothelial growth factor in vascular smooth muscle cells. FEBS Lett. *358*, 311–315.

Stone, J., and Dreher, Z. (1987). Relationship between astrocytes, ganglion cells and vasculature of the retina. J. Comp. Neurol. *255*, 35–49.

Stone, J., Itin, A., Alon, J., Pe'er, J., Gnessin, H., Chang-Ling, T., and Keshet, E. (1995). Development of retinal vasculature is mediated by hypoxia-induced vascular endothelial growth factor (VEGF) expression by neuroglia. J. Neurosci. *15*, 4738–4747.

Takakura, N., Yoshida, H., Kunisada, T., Nishikawa, S., and Nishikawa, S.-I. (1996). Involvement of platelet-derived growth factor receptor-α in hair canal formation. J. Invest. Dermatol., *107*, 770–777.

Tong, B.D., Auer, D.E., Jaye, M., Kaplow, J.M., Ricca, G., McConathy, E., Drohan, W., and Deuel, T.F. (1987). cDNA clones reveal differences between human glial and endothelial cell platelet-derived growth factor A-chains. Nature *328*, 619–621.

Turner, D.L., and Cepko, C.L. (1987). A common progenitor for neurons and glia persists in rat retina late in development. Nature *328*, 131–136.

Turner, D.L., Snyder, E.Y., and Cepko, C.L. (1990). Lineage-independent determination of cell type in the embryonic mouse retina. Neuron *4*, 833–845.

Uchihori, Y., and Puro, D.G. (1991). Mitogenic and chemotactic effects of platelet-derived growth factor on human retinal glial cells. Invest. Ophthalmol. Vis. Sci. *32*, 2689–2695.

Uren, A., Yu, J.C., Gholami, N.S., Pierce, J.H., and Heidaran, M.A. (1994). The alpha PDGFR tyrosine kinase mediates locomotion of two different cell types through chemotaxis and chemokinesis. Biochem. Biophys. Res. Commun. *204*, 628–634.

Watanabe, T., and Raff, M.C. (1988). Retinal astrocytes are immigrants from the optic nerve. Nature *332*, 834–837.

Wetts, R., and Fraser, S.E. (1988). Multipotent precursors can give rise to all major cell types of the frog retina. Science *239*, 1142–1145.

Yu, J.C., Mahadevan, D., LaRochelle, W.J., Pierce, J.H., and Heidaran, M.A. (1994). Structural coincidence of alpha PDGFR epitopes binding to platelet-derived growth factor-AA and a potent neutralizing antibody. J. Biol. Chem. *269*, 10668–10674.